

# Acoustic plasmons and isotropic short-range interaction in two-component electron liquids

A. N. Afanasiev\*  
*Ioffe Institute, St. Petersburg 194021, Russia*

Collective density excitation spectrum in two-component electron liquids is dominated by conventional optical plasmon at high frequencies and charge neutral gapless acoustic mode in the quasi-classical domain. In this work we reveal the identity between the latter acoustic plasmon and zero sound propagating in the slow component. Within the framework of two coupled collisionless Landau-Silin kinetic equations with the microscopically calculated isotropic Landau parameters we show that the intercomponent screening plays a key role in description of collective modes and quasiparticle interaction in two-component electron liquids. It is responsible for the stability of acoustic plasmon to the long-range electrostatic interaction and suppresses the mode renormalization by the short-range exchange-correlation interactions. The acoustic plasmon mediated Fröhlich-like interparticle effective interaction in the fast component is weak in both the three- and two-dimensional electron liquids with parabolic dispersion and the associated plasmonic superconductivity and the formation of acoustic plasmaron are subjects of anisotropic multiband systems with linear dispersion like type-I Weyl semimetals.

## I. INTRODUCTION

The concept of elementary excitations in interacting systems, originally introduced by L. D. Landau [1, 2] to describe the low-energy properties of the Fermi liquid, plays a key role in condensed matter physics. In particular, collective modes which represent the bosonic part of the excitation spectra are well-known to be responsible for various electronic and structural properties of condensed matter systems [3, 4].

The recent demonstration of the strongly interacting electron liquid and Dirac fluid behavior in high-quality samples of graphene [5, 6], quasi-two dimensional metals [7] and GaAs quantum wells [8] manifesting in the hydrodynamic regime of electron transport has stimulated an extensive research on the collective mode structure of such systems. Novel hydrodynamic and collisionless electronic sound modes were predicted in Dirac fluids [9–11] and gated two-dimensional electron liquids [12]. However, the spectrum of collective density excitations of electron liquids is consistent with the fundamental result of Landau-Silin theory [13, 14]: in the long-wavelength domain long-range coulomb interaction transforms both the collisionless zero sound [13] and the hydrodynamic first sound [15, 16] into plasmons [17]. Sound modes supported by electron liquid are associated with anisotropic part of the short-range quasiparticle interaction described by high-order Landau parameters  $F_n$ ,  $n \geq 1$  [14, 18–21]. Namely, propagation of the shear sound [22–26] determined by the dipole Landau interaction manifests in the the viscoelastic resonance in highly viscous electron fluids. Absence of density oscillation in this mode provides immunity to coulomb interaction, but also makes it inaccessible by standard charge-sensitive experimental techniques [27–29].

The spectrum of collective density oscillations of two-component electron systems is qualitatively different. In high-density two-component degenerate electron gas, the ordinary high-frequency *optical* plasma mode is accompanied by *acoustic plasmon* in quasi-classical domain, see Fig. 1. The character of density oscillations in this mode is similar to zero sound in neutral Fermi liquids [2, 30]: the total charge variation in the vibration is zero since the partial contributions of components compensate each other (Fig. 1). Consequently, the mode has gapless linear dispersion and its velocity is between the Fermi velocities of the slow and the fast components. Predicted long ago by D. Pines [31], acoustic plasmons were considered to be a source of unconventional, purely electronic superconductivity in multiband materials such as transition metals with incomplete inner shell [32], electron-hole liquids [33, 34], graphene/transition metal dichalcogenide bilayers [35], bismuth [36] and layered materials such as twisted bilayer graphene [37]. Another manifestation of this mode is the spin plasmon in two-dimensional degenerate gases with spin splitting [38–42].

At low densities, modification of acoustic plasmon dispersion in two-component electron liquids was studied within generalized random phase approximation in Refs. [43, 44]. Zero sound in two-component charged Fermi liquids was considered separately in the framework of Landau-Silin theory [45–47] and no connection between these two modes has been established yet.

In this work we show that two-component electron liquids support zero sound mode in the form of acoustic plasmon in three and two dimensions. In Section II we formulate the system of macroscopic collisionless Landau-Silin kinetic equations and show that acoustic plasmon is identical to zero sound propagating in the slow component thanks to the screening of long-range intracomponent Coulomb interaction by the fast quasiparticles. The corresponding density oscillations in the slow component are described by the characteristic zero sound-like deformation of the slow Fermi

\* afanasiev.an@mail.ru

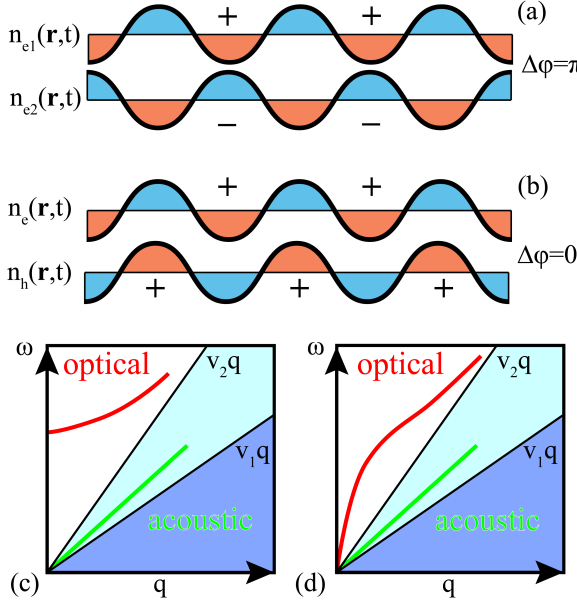


FIG. 1. Schematic representation of acoustic plasmon mode in two-component electron liquids. Panels (a) and (b) demonstrate the characteristic density (black solid lines) and charge (marked by color) variations in the vibration in electron-electron and electron-hole liquid, respectively. Panels (c) and (d) demonstrate schematic plasmon dispersions and particle-hole continuum domains in three and two dimensions.

surface (Sec. III A) and the fast Fermi surface acquires Čerenkov cone features due to Landau damping. When the effective Landau parameter is small, acoustic plasmon dispersion and the deformation of the Fermi surface in the slow component resemble zero sound in almost ideal Fermi gas (Sec. III B). With increase of the effective interaction strength, acoustic mode continuously transforms into ion-acoustic wave – Pines plasmon [31]. Next, in Section IV we calculate the isotropic Landau parameters of the two-component electron liquid determined by the short-range exchange-correlation interaction between quasiparticles. In Section V we apply the microscopically calculated Landau parameters to macroscopic theory of Section II to determine the renormalization of acoustic plasmons. The strength of the acoustic plasmon mediated electron-electron interaction in the fast component and the case of type-I Weyl semimetals are discussed in Section VI.

## II. EQUIVALENCE OF ACOUSTIC PLASMON AND ZERO SOUND

We consider isotropic, non-polarized system with two types of degenerate carriers with parabolic dispersion. Each component is characterized by elementary charge  $e_\alpha = \pm e$ , mass  $m_\alpha$  and Fermi wave vector  $k_\alpha$ . Hereinafter, indices  $\alpha = 1, 2$  and  $\beta = 1, 2$  denote the components of electron liquid. The evolution of the nonequi-

librium quasiparticle distributions in components associated with propagation of acoustic plasmon is described by the the pair of two coupled collisionless Landau-Silin kinetic equations [2, 14, 30] of the form

$$\frac{\partial n_\alpha}{\partial t} + \frac{\partial \mathcal{E}_\alpha}{\partial \mathbf{p}} \frac{\partial n_\alpha}{\partial \mathbf{r}} - \frac{\partial \mathcal{E}_\alpha}{\partial \mathbf{r}} \frac{\partial n_\alpha}{\partial \mathbf{p}} = 0 \quad (1)$$

where  $n_\alpha(\mathbf{r}, \mathbf{p}, t)$  is the nonequilibrium occupation number and the quasiparticle energies  $\mathcal{E}_\alpha(\mathbf{r}, \mathbf{p}, t) = \mathcal{E}_\alpha[n_1, n_2]$  are functionals of  $n_\alpha(\mathbf{r}, \mathbf{p}, t)$  given by

$$\mathcal{E}_\alpha(\mathbf{r}, \mathbf{p}, t) = \epsilon_\alpha(\mathbf{p}) + U_\alpha(\mathbf{r}, \mathbf{p}, t) + E_\alpha(\mathbf{r}, \mathbf{p}, t), \quad (2)$$

$$U_\alpha(\mathbf{r}, \mathbf{p}, t) = \sum_{\beta \neq \alpha} \frac{e_\alpha e_\beta}{\varkappa |\mathbf{r} - \mathbf{r}'|} n_\alpha(\mathbf{r}, \mathbf{p}, t) \delta N_\beta(\mathbf{r}', t), \quad (3)$$

$$E_\alpha(\mathbf{r}, \mathbf{p}, t) = \sum_{\beta \neq \alpha} f_s^{\alpha\beta}(\vartheta) \delta n_\beta(\mathbf{r}, \mathbf{p}', t), \quad (4)$$

where  $\epsilon_\alpha(\mathbf{p})$  is the bare energy of non-interacting fermions,  $U_\alpha(\mathbf{r}, \mathbf{p}, t)$  is the potential energy in the self-consistent electrostatic field and  $E_\alpha(\mathbf{r}, \mathbf{p}, t)$  is the energy renormalization by the spin-symmetric part of short-range Landau interaction between quasiparticles,  $\delta N_\alpha(\mathbf{r}', t)$  stands for the nonequilibrium concentration,  $\varkappa$  is the background dielectric constant and  $\sum_{\mathbf{r}'} = \int d\mathbf{r}'$ . In isotropic systems, Landau interaction function depends only on the angle  $\vartheta = \widehat{\mathbf{p}\mathbf{p}'}$  between momenta of interacting quasiparticles. In two-component electron liquids the diagonal elements of  $f_s^{\alpha\beta}(\vartheta)$  describe the intracomponent short-range interaction at the Fermi surfaces, while the non-diagonal ones describe intercomponent interaction.

Following Landau-Silin theory of electron liquid [2, 14, 30], we describe the weakly excited state of two-component electron liquid in terms of the deformed Fermi surfaces  $\mathcal{E}_F^{(\alpha)}(\mathbf{r}, \mathbf{p}, t) = \mu_\alpha + \Phi_\alpha(\mathbf{r}, \mathbf{p}, t)$  in components, where  $\mu_\alpha$  is the equilibrium Fermi energy and  $\Phi_\alpha(\mathbf{r}, \mathbf{p}, t) \ll \mu_\alpha$  is the Fermi surface deformation. Hence the occupation numbers take the form

$$n_\alpha(\mathbf{r}, \mathbf{p}, t) \approx n_0^{(\alpha)}(\mathbf{p}) + \Phi_\alpha(\mathbf{r}, \mathbf{p}, t) \delta(\mu_\alpha - \epsilon_\alpha(\mathbf{p})), \quad (5)$$

where  $n_0^{(\alpha)}(\mathbf{p})$  is the equilibrium distribution. Therefore, kinetic equations (1) can be linearized and reduced to equations for the Fermi surface deformation. According to (5), quasiparticles are excited only from the Fermi surface and the deformation  $\Phi_\alpha(\mathbf{r}, \mathbf{p}_\alpha, t) = \Phi_\alpha(\mathbf{r}, \mathbf{e}_\mathbf{p}, t)$  depends only on the direction of Fermi velocity  $\mathbf{v}_\alpha = \nabla_{\mathbf{p}} \epsilon_\alpha(\mathbf{p}_\alpha)$ , where  $p_\alpha = \hbar k_\alpha$  denotes the Fermi momentum.

Microscopic calculations show that the spin-symmetric Landau interaction function in the single-component electron liquids is almost isotropic [48, 49]. Namely, dimensionless isotropic Landau parameter  $F_0$  is greater than the dipole parameter  $F_1$  and the other high-order ones by an order of magnitude in both the three and two dimensions. In this work we consider the effect of isotropic part of the short-range quasiparticle interaction on acoustic plasmons in two-component. Consequently,

Landau interaction function in (4) is approximated by  $f_s^{\alpha\beta}(\vartheta) \approx D_\beta^{-1} F_0^{\alpha\beta}$  and we neglect the interaction-induced renormalization of mass and the density of states at the Fermi surfaces  $D_\beta = D_d(\mu_\beta)$ . Emergence of transverse zero sound in two-component electron liquids associated with  $F_1^{\alpha\beta}$  was considered in [50].

The propagation of acoustic plasmon is accompanied by the plane wave-like deformation of the Fermi surfaces in components. Taking into account the linear dispersion of the mode  $\omega_{\text{ac}}(k) = sk$  where  $s$  is the velocity of sound, expression for  $\Phi_i(\mathbf{r}, \mathbf{e}_p, t)$  takes the form

$$\Phi_\alpha(\mathbf{r}, \mathbf{p}, t) = \Phi_s^{(\alpha)}(\theta) e^{i(\mathbf{k}\mathbf{r} - skt)} \quad (6)$$

where  $\theta$  is the angle between  $\mathbf{e}_p$  and the direction of the wave propagation  $\mathbf{k}/k$ . Combining Eqs. (6) and (5) with (3), (4) and (1), we come to important result that the propagation of acoustic plasmon, i.e. its velocity and the shape of the oscillating Fermi surfaces, is governed by the system of two coupled integral equations

$$\left( \frac{s}{v_\alpha} - \cos \theta \right) \Phi_s^{(\alpha)}(\theta) = \cos \theta \int \frac{d\Omega'}{\Omega_d} F^{\alpha\beta}(k) \Phi_s^{(\beta)}(\theta'), \quad (7)$$

where  $\Omega_d = \int d\Omega'$  is the  $d$ -dimensional solid angle and the summation over repeated indices is assumed. The system (7) reproduces the form of zero sound equations in two-component Fermi liquids [45–47] with the isotropic  $k$ -dependent Landau parameters renormalized [14–16] by the long-range coulomb interaction

$$F^{\alpha\beta}(k) = F_0^{\alpha\beta} + F_c^{\alpha\beta}(k), \quad (8)$$

$$F_c^{\alpha\beta}(k) = D_\beta V_{\alpha\beta}(k) = \frac{e_\alpha}{e_\beta} \left( \frac{\kappa_\beta}{k} \right)^{d-1}, \quad (9)$$

where  $\kappa_\alpha$  denote the Thomas-Fermi wave vectors in components and the Fourier transform of coulomb interaction in three and two dimensions is  $V_{\alpha\beta}(k) = 4\pi e_\alpha e_\beta / \pi k^2$  and  $V_{\alpha\beta}(k) = 2\pi e_\alpha e_\beta / \pi k$ , respectively. Explicit expressions for the complex amplitudes of the Fermi surfaces deformation following from (6) are

$$\Phi_s^{(\alpha)}(\theta) = \frac{e_\alpha}{e} \frac{\cos \theta}{s/v_\alpha - \cos \theta} U_s, \quad (10)$$

where  $U_s$  is the complex amplitude of the self-consistent potential in the vibration.

The corresponding equation for the acoustic plasmon velocity

$$F_c^{11}(k) \bar{\Pi}_1(s) + F_c^{22}(k) \bar{\Pi}_2(s) = 0, \quad (11)$$

can be formulated in terms of the dimensionless proper polarizabilities

$$\bar{\Pi}_\alpha(s) = \frac{\tilde{\Pi}_\alpha(s)}{1 - \tilde{F}_0^{\alpha\alpha} \tilde{\Pi}_\alpha(s)}, \quad (12)$$

determined by the dimensionless non-interacting quasi-classical polarizabilities  $\tilde{\Pi}_\alpha(s) = \Pi_\alpha(s)/D_\alpha$  and the reduced Landau parameters

$$\tilde{F}_0^{\alpha\alpha} = F_0^{\alpha\alpha} - \frac{e_\alpha}{e_\beta} F_0^{\beta\alpha}, \alpha \neq \beta. \quad (13)$$

The dispersion equation (11) has two possible solutions. First of them lies beyond the particle-hole continua of components and its velocity is greater than both the velocities of the slow (first) and the fast (second) carriers. This is a conventional zero sound mode [45–47] analogous to the case of single component neutral Fermi liquid. However, this branch arises only when the reduced short-range interaction  $\tilde{F}_0^{\alpha\alpha}$  is repulsive in both components. As it will be shown in Section IV, this is not the case of two-component electron liquids, thus this mode is absent. Velocity of the second branch lies between the slow and the fast Fermi velocities. This is an acoustic plasmon mode, which is a special case of zero sound in two-component electron liquids. Acoustic plasmon velocity determined by Eq. (11) coincides with the one given by the zero of the quasi-classical dielectric function of two-component electron liquid

$$\varepsilon(sk, k) = 1 - V(k) \bar{\chi}_1(s) - V(k) \bar{\chi}_2(s), \quad (14)$$

$$\bar{\chi}_\alpha(s) = D_\alpha \tilde{\Pi}_\alpha(s) \frac{1 - \tilde{F}_0^{\beta\beta} \tilde{\Pi}_\beta(s)}{1 - F_0^{11} \tilde{\Pi}_1(s) - F_0^{22} \tilde{\Pi}_2(s)}, \alpha \neq \beta. \quad (15)$$

Here  $V(k) = V_{\alpha\alpha}(k)$  and  $\bar{\chi}_\alpha(s)$  denotes the proper density response function. Eq. (11) indicates that the mode carries zero total charge density  $\delta\rho_s = e_1 \delta N_s^{(1)} + e_2 \delta N_s^{(2)} = 0$  in the long-wavelength domain. The phase shift between the complex amplitudes of the density oscillations in components  $\delta N_s^{(\alpha)} = e_\alpha \bar{\chi}_\alpha(s) U_s$  dictated by the long-range intra- and intercomponent coulomb interaction depends on the charge composition of electron liquid

$$\delta N_s^{(1)} = -\frac{e_2}{e_1} \delta N_s^{(2)}. \quad (16)$$

Density oscillations are out-of-phase in the case of electron-electron liquid and in-phase in electron-hole liquid, see Fig. 1a,b.

Since acoustic plasmon velocity is between the slow and the fast Fermi velocities, the mode is affected by Landau damping [51] due to the intraband single particle transitions in the fast component. Therefore acoustic plasmon frequency acquires imaginary part and we treat it in terms of the complex velocity  $s = s' - is''$ , where the correct sign of  $s'' > 0$  correspond to decay of the charge density oscillations in time. Well-defined acoustic plasmon with  $s''/s' \ll 1$  arises when the difference in the Fermi velocities is great  $v_2/v_1 \gg 1$  implying that the liquid components are weakly coupled. Taking into account an approximate form of the polarizability  $\text{Re } \tilde{\Pi}_2(s') = -1$

at  $s'/v_2 \rightarrow 0$ , the dispersion equation (11) transforms into

$$\Pi_1(s') = \frac{1}{F_{\text{eff}}}, \quad (17)$$

indicating that in this regime acoustic plasmon is identical to the zero sound [30] propagating in the slow component with the effective interaction parameter

$$F_{\text{eff}} = (1 + \tilde{F}_0^{22})F_{\text{RPA}} + \tilde{F}_0^{11}. \quad (18)$$

Note that  $\tilde{\Pi}_1(s')$  is real-valued function at  $s' > v_1$ . This special case of zero sound does not vanish in the high-density regime, when the short range interaction is absent  $F_0^{\alpha\beta} \rightarrow 0$  and Eqs. (11), (14) and (15) reproduce the results for the quasi-classical limit of RPA. The effective interaction parameter Eq. (18) in RPA is given by the coulomb interaction in the slow component at the Thomas-Fermi wave vector of the fast component  $F_{\text{RPA}} = F_c^{11}(\kappa_2) = (\kappa_1/\kappa_2)^{d-1}$ . This reveals the reason why the acoustic plasmon-zero sound mode is stable to the long-range coulomb interaction: particles of the fast component screen out the intracomponent interaction in the slow one, making it effectively short-range. However, the mode stabilization inevitably leads to the finite lifetime of this collisionless zero sound mode introduced by the particle-hole excitations in the fast component

$$s'' \approx \frac{F_{\text{RPA}}}{F_{\text{eff}}^2} \frac{\text{Im} \Pi_2(s')}{\partial \text{Re} \Pi_1(s')/\partial s}. \quad (19)$$

### III. STRUCTURE OF THE ACOUSTIC PLASMON MODE

#### A. Shape of the Fermi surfaces in acoustic plasmon mode

Now we turn to investigation of the internal structure of the acoustic plasmon and consider the shape of the Fermi surfaces which oscillate as the mode propagates. Since the acoustic plasmon velocity has both real and imaginary parts, we use real representations of  $\Phi_\alpha(\mathbf{r}, \theta, t) = \text{Re}(\Phi_s^{(\alpha)}(\theta)e^{-s''kt}e^{i(\mathbf{kr}-s'kt)})$  to study the angular dependence of the Fermi surfaces. As it is shown in Fig. 2, Landau damping (i.e.  $s'' \neq 0$ ) not only provides the exponential decay of  $\Phi_{1,2}$  but also sufficiently affects the shape of the Fermi surface in the fast component. Nonzero  $s''$  regularize singularities in  $\Phi_2$  at  $\cos \theta = s'/v_2$  signifying excitation of quasiparticles of the fast component which move in phase with the wave. This resonant condition correspond to the inverse Čerenkov effect [51] which underlies Landau damping. The resulting shape of  $\mathcal{E}_F^{(1,2)}(\mathbf{r}, \theta, t)$  resemble the Čerenkov cone indicating the propagation of the shock wave of the fast Fermi surface deformation in the energy space.

In the case of the slow component, Čerenkov pole is absent since  $s' \geq v_1$  and the influence of Landau damping on the shape of  $\Phi_s^{(1)}(\theta)$  is negligible when  $s''/s' \ll 1$ .

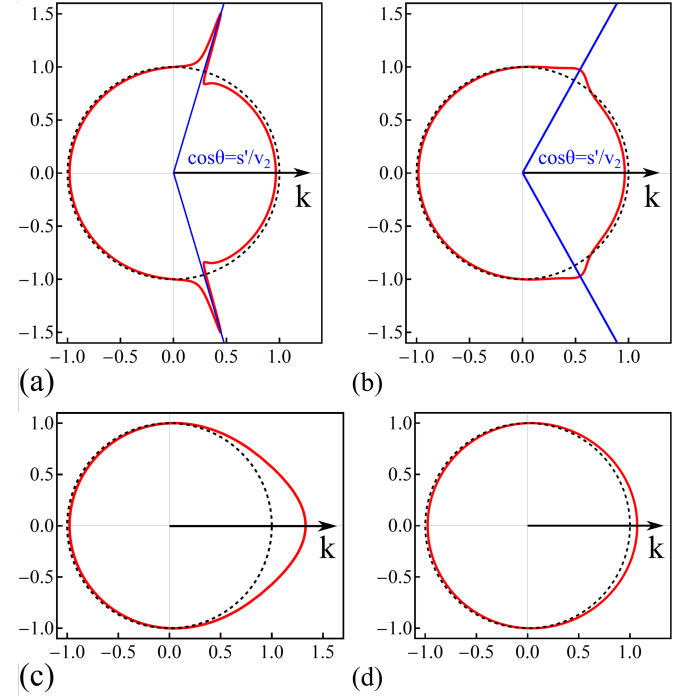


FIG. 2. Shapes of the Fermi surfaces in the fast (a,b) and the slow (c,d) components of the electron-electron liquid corresponding to acoustic plasmon propagation in (a,c) the regime of zero sound in the almost ideal Fermi gas given by Eqs. (22) and (29) at  $s'/v_1 = 1.1$  and (b,d) the ion-acoustic wave regime after Eqs. (24) and (31) at  $s'/v_1 = 2$ . Red curves denote the cross-section of the deformed Fermi surfaces  $\mathcal{E}_F^{(1,2)}(\mathbf{r}, \mathbf{p}, t)/\mu_{1,2}$  as a function of  $\mathbf{e}_p$  with respect to plasmon wave vector  $\mathbf{k}$  and the dashed black circles correspond to the equilibrium case. The  $\mathbf{kr} - \omega t = 7\pi/4$  wave plane is chosen and  $\text{Re} U_s/\mu_2 = 0.035$ ,  $\mu_2/\mu_1 = 2$ ,  $v_2/v_1 = 4$ ,  $s''/v_2 = 0.05$ .

Therefore the shape of the slow Fermi surface given by [52]

$$\Phi_1(\mathbf{r}, \theta, t) = U_s e^{-s''kt} \frac{\cos \theta}{s'/v_1 - \cos \theta} \cos(\mathbf{kr} - s'kt) \quad (20)$$

is similar to the case of zero sound propagation in single component neutral Fermi liquid and the degree of the slow Fermi surface distortion depends on the relation between  $s'$  and  $v_1$ .

#### B. Acoustic plasmon velocity and damping in three and two dimensions

Now we consider explicit solutions for acoustic plasmon velocity  $s'$  and damping  $s''$  determined by the specific form of  $\tilde{\Pi}_\alpha(s)$  for three and two dimensions. In the three-dimensional case the quasi-classical polarizability has the form (see Fig. 3a)

$$\tilde{\Pi}(s) = -1 - \frac{s}{2v_F} \ln \left( \frac{s - v_F}{s + v_F} \right) \quad (21)$$

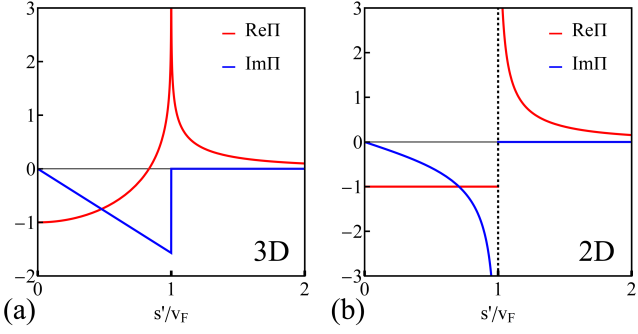


FIG. 3. Dimensionless quasi-classical polarizabilities in three and two dimensions after Eqs. (21) and (26).

and the general equation (11) has solution if both  $v_2/v_1$  and  $\mathcal{F}_{\text{eff}}$  exceed threshold values. Eq. (17) has no general analytic solution in three dimensions so we focus on its limiting cases. When the effective interaction is weak  $\mathcal{F}_{\text{eff}} \ll 1$ , acoustic plasmon velocity coincides with the velocity of zero sound in the almost ideal Fermi gas [30]

$$s' = v_1 \left( 1 + 2e^{-2/F_{\text{eff}}} \right) \quad (22)$$

$$\frac{s''}{s'} = 2\pi \frac{F_{\text{RPA}}}{F_{\text{eff}}^2} \frac{v_1}{v_2} e^{-2/F_{\text{eff}}}. \quad (23)$$

The propagation of the mode in this regime is accompanied (see Fig. 2c) by the characteristic sufficient deformation of the slow Fermi surface towards  $\mathbf{k}$  [30] since  $s'$  is close to  $v_1$ . In this regime the damping of the mode is small due to the both  $v_2/v_1 \gg 1$  and  $F_{\text{eff}} \ll 1$ .

In the opposite case of strong interaction  $F_{\text{eff}} \gg 1$  acoustic plasmon mode is described by Pines plasmon [31] which is a solid state analogy of the ion-acoustic wave [51] with

$$s' = v_1 \sqrt{\frac{F_{\text{eff}}}{3}} \quad (24)$$

$$\frac{s''}{s'} = \frac{\pi}{4} \sqrt{\frac{F_{\text{RPA}}}{3F_{\text{eff}}}} \frac{v_1}{v_2}. \quad (25)$$

In this regime  $v_1 \ll s' \ll v_2$  and the Fermi surface only slightly differs from the equilibrium one as presented in Fig. 2c.

In the case of two dimensions the polarizability has the form (see Fig. 3b)

$$\tilde{\Pi}(s) = -1 + \text{sign}(\text{Re } s) \frac{s}{\sqrt{s^2 - v_F^2}}. \quad (26)$$

and the existence of solution of the general equation (11) is independent of the ratio  $v_2/v_1$  [44]. Acoustic plasmon velocity is similar to the zero sound velocity in two dimensions

$$s' = v_1 \frac{1 + F_{\text{eff}}}{\sqrt{1 + 2F_{\text{eff}}}}, \quad (27)$$

$$\frac{s''}{s'} = \frac{F_{\text{RPA}}}{F_{\text{eff}}^2} \frac{(s'^2 - v_1^2)^{3/2}}{v_1^2 \sqrt{v_2^2 - s'^2}}. \quad (28)$$

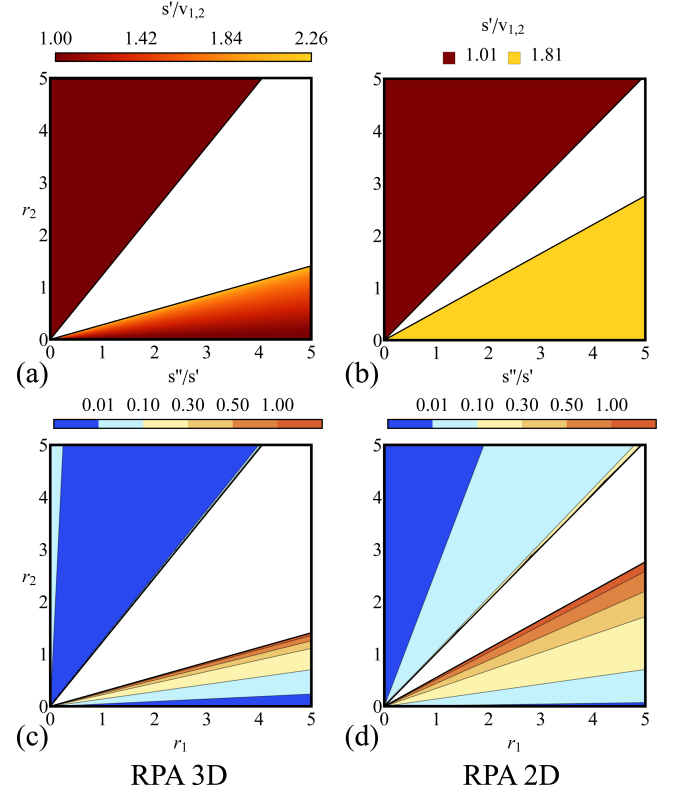


FIG. 4. Diagrams of acoustic plasmon velocity (a,b) and damping (c,d) within random phase approximation in three and two dimensions for  $m_2/m_1 = 0.2$ .

In the weak interaction regime  $F_{\text{eff}} \ll 1$

$$s' = v_1 \left( 1 + \frac{1}{2} F_{\text{eff}}^2 \right), \quad (29)$$

$$\frac{s''}{s'} = F_{\text{RPA}} F_{\text{eff}} \frac{v_1}{\sqrt{v_2^2 - v_1^2}}, \quad (30)$$

and acoustic plasmon is well defined if the Fermi velocities of components are far from the resonance  $v_2 \neq v_1$ . In the strong interaction case  $F_{\text{eff}} \gg 1$

$$s' = v_1 \sqrt{\frac{F_{\text{eff}}}{2}}, \quad (31)$$

$$\frac{s''}{s'} = \frac{F_{\text{RPA}}}{F_{\text{eff}}} \frac{s'}{2\sqrt{v_2^2 - s'^2}}, \quad (32)$$

and the damping is small when  $s'/v_2 \ll 1$ .

Possibility and the particular regime of acoustic plasmon propagation in two-component electron liquid characterized by the specific set of parameters, namely, elementary charges of carriers  $e_{1,2}$ , mass ratio  $m_2/m_1$  and dimensionless Wigner-Seitz radii  $r_{1,2}$  depend on the approximation used for the effective interaction parameter  $F_{\text{eff}}$  or, more generally, for parameters in the dispersion equation (11). From now on, indices 1 and 2 are used only for numeration of components. Since  $v_2/v_1 = r_1/r_2$ , the

theory developed above can be readily applied for  $r_1 > r_2$  and the index permutation  $1 \leftrightarrow 2$  is needed at  $r_2 > r_1$ .

In RPA, propagation of acoustic plasmon is controlled by the ratio of the Thomas-Fermi wave vectors in components  $\delta\kappa = \kappa_2/\kappa_1$ . Therefore, the case of strong effective interaction is realized when the screening by the fast component is weak and vice versa. Within RPA, acoustic plasmons are equivalent in electron-electron and electron-hole liquids. Diagrams of the numerically calculated acoustic plasmon velocity and damping according to Eqs. (11) and (19) at  $F_0^{\alpha\beta} = 0$  and  $m_2/m_1 = 0.2$  are presented in Fig. 4. In the central parts of the diagrams at  $r_2 \sim r_1$  there is a forbidden domain where acoustic plasmons do not propagate. The difference in the sizes of the forbidden domains in two and three dimensions is related to different behavior of  $\text{Re}\tilde{\Pi}(s)$  for  $s' < v_F$  in 3D and 2D (see Fig. 3).

In three dimensions, the RPA effective interaction parameter  $F_{\text{RPA}} = m_1^2 r_2 / m_2^2 r_1$  (for  $r_1 > r_2$ ) depends on the ratios of masses and interaction constants. At fixed  $m_2/m_1 < 1$ , the effective interaction is increased (in comparison to the  $m_1 = m_2$  case) in the lower parts of Figs. 4a,c and decreases when  $r_2 > r_1$ . In the quasi-single component regions  $r_{1,2} \ll 1$ ,  $F_{\text{RPA}}$  is small due to strong screening by high-density component. Therefore, in the upper domains of the diagrams shown in Fig. 4a,c acoustic plasmon propagates in the regime of zero sound in the almost ideal Fermi liquid (22). In the lower domains, the effective interaction could be strong near the edge of the forbidden region, far away from the domain of strong screening. However, at the edge of the forbidden domains, acoustic plasmon acquire infinite damping and the mode becomes well-defined with the increase of the Fermi velocities difference. Consequently, the ion-acoustic wave regime (24) is suppressed in three-dimensional two-component electron liquids even within RPA.

The effective interaction parameter in two dimensions is determined solely by the mass ratio  $F_{\text{RPA}} = m_1/m_2$  (for  $r_1 > r_2$ ). Acoustic plasmon velocity is hence constant in the lower and upper parts of the diagram (Fig. 4b) and both the well-defined zero sound in the almost ideal Fermi liquid (29) and Pines plasmon (31) regimes take place at  $r_2 \gg r_1$  and  $r_2 \ll r_1$ , respectively, provided the mass difference is strong.

As we have seen above, propagation of acoustic plasmon is favorable when the interaction constants in components are strongly different. Therefore, it is essential to take into account the quasiparticle short-range interaction to study the acoustic plasmon dispersion and damping in two-component electron liquids. Renormalization of the acoustic plasmon mode and the modification of the RPA diagrams is determined by the behavior of the isotropic Landau parameters in the  $r_1 - r_2$  plane

$$F_0^{\alpha\beta} = F_0^{\alpha\beta}(\delta m, r_1, r_2), \quad (33)$$

where  $\delta m = m_2/m_1$ .

#### IV. MICROSCOPIC CALCULATION OF ISOTROPIC LANDAU PARAMETERS

Short-range quasiparticle interaction in electron liquids is associated with particle exchange and coulomb correlations. Landau interaction function in two-component electron liquid is defined in the similar manner to the single-component case as a functional derivative of quasiparticle energy with respect to quasiparticle occupation number at Fermi surfaces

$$f_{\sigma\sigma'}^{\alpha\beta}(\vartheta) = \frac{\delta\mathcal{E}_\alpha^\sigma(\mathbf{k})}{\delta n_{\beta'}^\sigma(\mathbf{k}')} \bigg|_{\substack{\mathbf{k}=\mathbf{k}_\alpha \\ \mathbf{k}'=\mathbf{k}'_\beta}}, \quad (34)$$

where  $\vartheta = \widehat{\mathbf{k}_\alpha \mathbf{k}'_\beta}$  is the angle between wave vectors of quasiparticles at Fermi surfaces,  $\sigma$  and  $\sigma'$  are spin projections. Microscopic calculation of  $f_{\sigma\sigma'}^{\alpha\beta}(\vartheta)$  is based on (34) and the particular form of the interaction induced renormalization of single particle spectrum within quantum field theory [49, 53–56].

In this work we use oh-shell approximation for quasiparticle energy given by

$$\mathcal{E}_\alpha^\sigma = \epsilon_\alpha^\sigma(\mathbf{k}) + \text{Re} \Sigma_\alpha^\sigma(\mathbf{k}, \epsilon_\alpha^\sigma(\mathbf{k})), \quad (35)$$

where  $\epsilon_\alpha^\sigma(\mathbf{k})$  is the energy dispersion of non-interacting fermions of type  $\alpha$ . The self energy  $\Sigma_\alpha^\sigma$  is calculated in  $G_0W$ -approximation

$$\Sigma_\alpha^\sigma(\mathbf{k}, \omega) = i \sum_{\mathbf{q}\omega'} W(\mathbf{q}, \omega') G_\alpha^\sigma(\mathbf{k} - \mathbf{q}, \omega - \omega'), \quad (36)$$

where  $\sum_{\mathbf{q}\omega'} = (2\pi)^{-d-1} \int d\mathbf{q} d\omega'$ ,  $G_\alpha^\sigma(\mathbf{k}, \omega) = (\omega - \epsilon_\alpha^\sigma(\mathbf{k}) + i\eta_\mathbf{k})^{-1}$  is the Green function of non-interacting fermions and  $\eta_\mathbf{k} = \eta \text{sgn}(k - k_\alpha)$  is infinitesimal ( $\eta \rightarrow 0_+$ ). For the effective interaction  $W_{\alpha\beta}(\mathbf{q}, \omega)$  the random-phase approximation (RPA) is used

$$W(\mathbf{q}, \omega) = \frac{V(\mathbf{q})}{\varepsilon_{\text{RPA}}(\mathbf{q}, \omega)}, \quad (37)$$

where  $V(\mathbf{q})$  is the Fourier transform of the bare Coulomb interaction and RPA dielectric function has the form

$$\varepsilon_{\text{RPA}}(\mathbf{q}, \omega) = 1 - \sum_{\alpha\sigma} V(\mathbf{q}) \Pi_\alpha^\sigma(\mathbf{q}, \omega), \quad (38)$$

$$\Pi_\alpha^\sigma(\mathbf{q}, \omega) = -i \sum_{\mathbf{k}'\omega'} G_\alpha^\sigma(\mathbf{k}', \omega') G_\alpha^\sigma(\mathbf{q} + \mathbf{k}', \omega + \omega'). \quad (39)$$

Here  $\Pi_\alpha^\sigma(\mathbf{k}, \omega)$  is the non-interacting polarizability of the fermions of type  $\alpha$ .

We consider isotropic, non-polarized system with two types of fermions residing in the vicinity of extremums of two weakly overlapping parabolic bands. This is consistent with the band structure of transition metals with incomplete inner shell [32], photoexcited electron-hole liquids in pure semiconductors [49] and elemental bismuth [36]. Due to the different symmetries of band wave

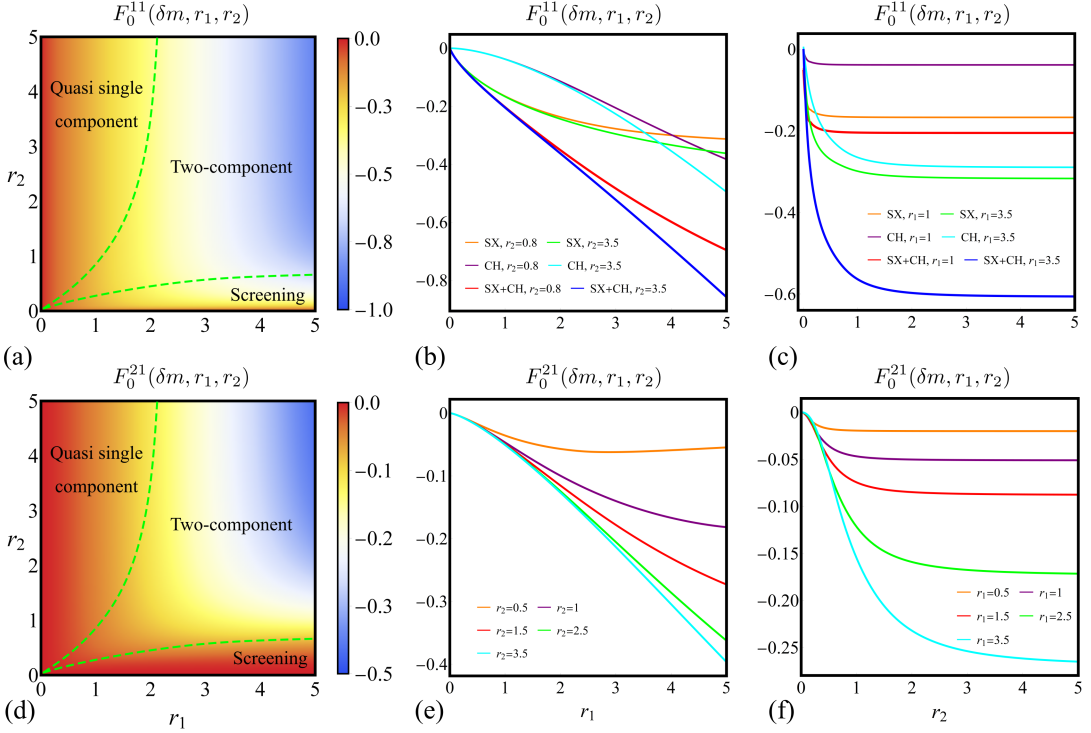


FIG. 5. Isotropic Landau parameters in three-dimensional two-component electron liquid at  $m_2/m_1 = 0.2$ . Panels (a) and (d) show the density plots of intracomponent and intercomponent parameters  $F_0^{11}$  and  $F_0^{21}$ . Their cuts and partial screened exchange (SX) and coulomb hole (CH) contributions at fixed  $r_1$  and  $r_2$  are presented on panels (b), (c), (e) and (f), respectively.

functions, overlap integrals are diagonal in component indices  $|\langle \alpha\sigma\mathbf{k}|\beta\sigma'\mathbf{k}'\rangle|^2 \approx \delta_{\alpha\beta}\delta_{\sigma\sigma'}$ , and the contribution of intercomponent transitions to the self energy (36) and RPA polarizability (39) is negligible. In the case of bismuth they are also accompanied by transfer of large wave vector comparable to the size of the Brillouin zone.

Using Eqs. (34), (35) and (36) we obtain the spin-symmetric part of the Landau interaction function  $f_s^{\alpha\beta} = (f_{\uparrow\uparrow}^{\alpha\beta} + f_{\uparrow\downarrow}^{\alpha\beta})/2$  given by two terms

$$f_s^{\alpha\beta}(\vartheta) = f_{\text{SX}}^{\alpha\beta}(\vartheta) + f_{\text{CH}}^{\alpha\beta}(\vartheta). \quad (40)$$

The first term is the screened exchange (SX) contribution

$$f_{\text{SX}}^{\alpha\beta}(\vartheta) = -\frac{1}{2}\delta_{\alpha\beta}W(\mathbf{k}_\alpha - \mathbf{k}'_\beta, 0), \quad (41)$$

determined by Pauli repulsion of non-interacting indistinguishable fermions with the same spin projection (exchange hole). Consequently, it is diagonal in components indices and proportional to the screened interaction at Fermi surface. The second term is the coulomb hole (CH) contribution determined by particle correlations due to coulomb interaction

$$f_{\text{CH}}^{\alpha\beta}(\vartheta) = -\text{Re} \sum_{\mathbf{q}\omega} W^2(\mathbf{q}, i\omega) G_\alpha(\mathbf{k}_\alpha - \mathbf{q}, \mu_\alpha - i\omega) \times \\ \times [G_\beta(\mathbf{k}'_\beta + \mathbf{q}, \mu_\beta + i\omega) + G_\beta(\mathbf{k}'_\beta - \mathbf{q}, \mu_\beta - i\omega)]. \quad (42)$$

It is second order by  $W(\mathbf{k}, \omega)$  and the both scattering processes at Fermi surfaces and outside them contribute to  $f_{\text{CH}}^{\alpha\beta}(\vartheta)$ . Intercomponent quasiparticle interaction is determined only by the coulomb hole term.

Equations (41) and (42) show that short-range exchange-correlation interaction in two-component electron liquids is attractive (similarly to the single-component case) and, in contrast to the long-range coulomb interaction, is independent of the signs of particles' charges. This asymmetry can be understood by qualitative comparison of correlation holes in electron-electron and electron-hole liquids. Electron-electron case is similar to the single-component one. Electron under scrutiny is surrounded by the depletion area of positive spatial charge due to intra- and intercomponent coulomb repulsion. The resulting short-range interaction with this correlation hole is attractive. In electron-hole liquids, vicinity of the electron under scrutiny is depleted with the other electrons and is populated by holes. Again, the correlation hole has positive effective charge and short-range interaction with it is attractive.

To obtain isotropic Landau parameters, interaction function (40) should be additionally averaged over the directions of  $\mathbf{k}'$  as  $F_0^{\alpha\beta} = D_\beta \sum_{\Omega_{\mathbf{k}'}} f_s^{\alpha\beta}(\vartheta)$ . Note that in (42) we have transformed the  $\omega$ -integration to imaginary axis [49, 53–56] to avoid plasmon poles and the poles of  $G_\alpha(\omega, \mathbf{k})$ . RPA dielectric function is real-valued at imaginary frequencies and is not associated with any

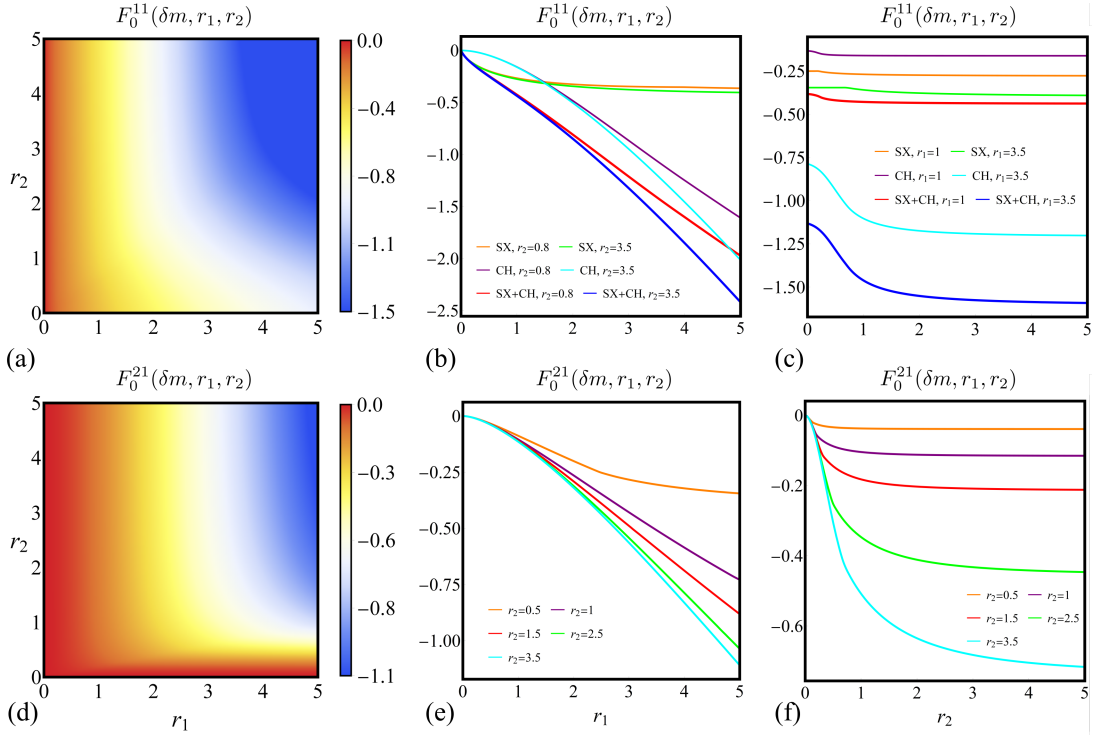


FIG. 6. Isotropic Landau parameters in two-dimensional two-component electron liquid at  $m_2/m_1 = 0.2$ . Panels (a) and (d) show the density plots of intracomponent and intercomponent parameters  $F_0^{11}$  and  $F_0^{21}$ . Their cuts and partial screened exchange (SX) and coulomb hole (CH) contributions at fixed  $r_1$  and  $r_2$  are presented on panels (b), (c), (e) and (f), respectively.

particle-hole and collective density excitations. Consequently, the only characteristic scale which determine the screening strength by the  $\alpha$  component is the Thomas-Fermi wave vector  $\kappa_\alpha$ . For isotropic system, angular integrations appearing in the coulomb hole term can be carried out analytically and the expressions for the screened exchange and the coulomb hole contributions to  $F_0^{\alpha\beta}$  take the final forms (A.1), (A.2) in 3D and (A.3), (A.4) in 2D suitable for numerical calculations.

As it is seen from the abovementioned formulas from the Appendix, the intra- and intercomponent Landau parameters are related by a simple permutation of the arguments

$$F_0^{22}(\delta m, r_1, r_2) = F_0^{11}(\delta m^{-1}, r_2, r_1), \quad (43)$$

$$F_0^{12}(\delta m, r_1, r_2) = F_0^{21}(\delta m^{-1}, r_2, r_1). \quad (44)$$

Consequently, further we will focus only on  $F_0^{11}$  and  $F_0^{21}$ .

At fixed mass ratio,  $r_1 - r_2$  plane is divided into several characteristic domains of quasiparticle interaction. In three dimensions, the ratio of Thomas-Fermi wave vectors  $\kappa_2/\kappa_1 = \delta m/\sqrt{\delta r_s}$  depends on the ratios of masses  $\delta m = m_2/m_1$  and interaction constants  $\delta r_s = r_2/r_1$ . Therefore, the relative screening strength of coulomb interaction at first Fermi surface induced by components varies with  $r_1$  and  $r_2$ . At high densities  $r_{1,2} \ll 1$ , isotropic Landau parameters take the following analytic

form when  $\kappa_2/\kappa_1 \lesssim 1$

$$F_{0,\text{SX}}^{11} = \frac{\gamma_3 r_1}{2\pi} \ln \left( \frac{\gamma_3 r_1 \kappa_1^2 + \kappa_2^2}{\pi \kappa_1^2} \right), \quad (45)$$

$$F_{0,\text{CH}}^{\alpha\alpha} = \frac{\gamma_3^2 r_\alpha^2}{\pi^2} \frac{m_1}{m_\alpha} \mathcal{I}_3 \left( \frac{r_\alpha}{r_1} \right) \ln \left( \frac{\gamma_3 r_1 \kappa_1^2 + \kappa_2^2}{\pi \kappa_1^2} \right), \quad (46)$$

where  $\gamma_3 = (4/9\pi)^{1/3}$  and  $\mathcal{I}_3(x) = 1/(1+x)$ . At low  $r_{1,2}$ , the screening length is greater than interparticle distance in components  $\lambda_{TF} \gg \lambda_F^\alpha$  and Landau parameters are determined by interaction at Fermi surfaces  $F_c^{\alpha\alpha}(k_\alpha) \sim r_\alpha$  and by coulomb logarithm associated with the screened processes of forward scattering. In a wider range of particle densities in components, Landau parameters can be calculated numerically using Eqs. (A.1) and (A.2). The results for  $m_2/m_1 = 0.2$  are demonstrated in Fig. 5. It can be clearly seen that the intercomponent interaction is comparable to the intracomponent one.

On the left sides of Figs. 5a and 5d, there is a region where  $\max[1, r_1] \kappa_2^2/\kappa_1^2 \ll 1$  (i.e.  $r_2 \gg \max[r_1, r_1^2] \delta m^2$ ) and the effective interaction in (A.1) and (A.2) is determined by screening by the high-density first component. As it follows from (45), (46) and Figs. 5b and 5c, intracomponent part of the short-range interaction  $F_0^{11}$  in this domain replicates the case of the isolated first component being almost independent of  $r_2$ . This quasi single component region is characterized by low  $r_1$  and, consequently,

weak quasiparticle interaction  $F_0^{11}, F_0^{21} \ll 1$  vanishing in the  $r_1 \rightarrow 0$  limit.

Two-component domain is characterized by comparable Thomas-Fermi wave vectors  $\kappa_2 \sim \kappa_1$ . In this region, RPA dielectric function is determined by the both components and the evolution of Landau parameters with  $r_{1,2}$  can be traced in terms of averaged interaction parameter  $\rho_s = \sqrt{r_1^2 + r_2^2}$ . In high density limit  $\rho_s \ll 1$  Landau parameters are described by Eqs. (45), (46) and the quasiparticle interaction is weak. With the decease of particle density  $\rho_s \geq 1$ , screening length becomes the shortest one  $\lambda_{TF} \ll \lambda_F^\alpha$  and the effective particle interaction at the Fermi surfaces is significantly reduced. Screened exchange term saturates at these densities while the absolute value of the coulomb hole one grows with  $\rho_s$  as it is determined by scattering processes outside the Fermi surfaces and dynamical screening, which is much weaker than the static one (see Appendix).

On the bottom of Figs. 5a and 5d, there is a screening domain at  $r_2 \ll \min[r_1, r_1^2] \delta m^2$ . Intra- and inter-component short-range interaction are weak (see Figs. 5c and 5f) due to strong screening by the high-density second component, which determines the RPA dielectric function. At  $r_1 \ll 1$ , isotropic Landau parameters in screening domain take the form

$$F_{0,\text{SX}}^{11} = -\frac{r_2}{2r_1} \frac{m_1^2}{m_2^2}, \quad (47)$$

$$F_{0,\text{CH}}^{11} = -0.6 \sqrt{\frac{\gamma_3}{\pi}} \frac{r_2^{3/2}}{\pi r_1} \frac{m_1^3}{m_2^3}, \quad (48)$$

$$F_{0,\text{CH}}^{21} = -1.2 \left(\frac{\gamma_3}{\pi}\right)^{3/2} \frac{r_2^{5/2}}{\pi r_1} \frac{m_1^2}{m_2^2}. \quad (49)$$

Both  $F_0^{11}$  and  $F_0^{21}$  vanish in the limit  $r_2 \rightarrow 0$ .

In two-dimensional case, the ratio of Thomas-Fermi wave vectors  $\kappa_2/\kappa_1 = m_2/m_1$  is determined by the mass difference only and the relative screening strength by components is constant in the whole  $r_1 - r_2$  plane. In the high density limit  $r_{1,2} \ll 1$ , Landau parameters take the form

$$F_{0,\text{SX}}^{\alpha\beta} = \delta_{\alpha\beta} \frac{\gamma_2 r_\alpha}{\pi} \ln \left( \gamma_2 r_\alpha \frac{\kappa_1 + \kappa_2}{\kappa_\alpha} \right), \quad (50)$$

$$F_{0,\text{CH}}^{\alpha\beta} = -\frac{\gamma_2^2 r_\alpha^2}{\pi^2} \frac{m_\beta}{m_\alpha} \mathcal{I}_2 \left( \frac{r_\alpha}{r_\beta} \right), \quad (51)$$

where  $\mathcal{I}_2(x) = \frac{2x}{(1-x^2)^2} [(1+x^2)K(1-x^2) - 2E(1-x^2)]$ ,  $K(x)$  and  $E(x)$  are the complete elliptic integrals of the first and second kinds [57], respectively and  $\gamma_2 = 1/\sqrt{2}$ . In contrast to the three-dimensional case, coulomb hole contribution in 2D is not affected by the coulomb logarithm. According to Eqs. (50) and (51), in two-component electron liquids intracomponent interaction qualitatively reproduce the single component case with constant renormalization controlled by the mass ratio. This is consistent with the results of numerical calculation of Landau parameters presented in Fig. 6.

As it is shown in Figs. 6a-c, the dependence of  $F_0^{11}$  on  $r_2$  is very weak and  $F_0^{11}$  is nonzero in the  $r_2 \rightarrow 0$  limit. The intercomponent Landau parameter  $F_0^{21}$  vanishes in the single-component limits  $r_{1,2} \rightarrow 0$  and its values are comparable to  $F_0^{11}$  at  $r_{1,2} \geq 1$ , see Figs. 6d-f. Similarly to the single-component case, short-range interaction is stronger in 2D than in 3D.

The remaining parameters  $F_0^{22}$  and  $F_0^{12}$  associated with the second component are of the same order as  $F_0^{11}$  and  $F_0^{21}$  when  $\delta m \approx 1$  and much smaller when  $\delta m \ll 1$ .

## V. RENORMALIZED ACOUSTIC PLASMONS

Now we can use the numerically calculated Landau parameters from the previous section to determine the acoustic plasmon renormalization in two-component electron liquids. The diagrams of acoustic plasmon velocity and damping given by Eq. (11) for the cases of electron-electron and electron-hole liquids with equal and strongly different masses in components are presented in Fig. 7 and Fig. 8 for 3D and 2D, respectively.

It is seen from Figs. 7 and 8 that acoustic plasmons in electron-electron and electron-hole liquids are non-equivalent [see the expression for the reduced Landau parameters (13) entering the dispersion equation (11)]. This is a direct consequence of the asymmetry of inter-component short-range interaction with respect to the sign of elementary charges of particles in components. This peculiarity can be qualitatively understood by considering the restoring forces  $\mathcal{F}_\alpha(\mathbf{r}, \mathbf{p}, t) = -\nabla_{\mathbf{r}} \mathcal{E}_\alpha(\mathbf{r}, \mathbf{p}, t)$  which act on the quasiparticles of type  $\alpha$  in the vibration. The complex amplitude of the partial contribution to  $\mathcal{F}_\alpha$  exerted due to density variation  $\delta N_s^{(\beta)}$  in the  $\beta$  component is

$$\mathcal{F}_{\omega\mathbf{k}}^{\alpha\beta} = -i\mathbf{k} \left[ V_{\alpha\beta}(k) + f_0^{\alpha\beta} \right] \delta N_s^{(\beta)}, \quad (52)$$

where  $f_0^{\alpha\beta}$  is the isotropic part of the Landau interaction function (40). In the long-wavelength domain the partial restoring force  $\mathcal{F}_{\omega\mathbf{k}}^{\alpha\beta}$  is dominated by the long-range electrostatic interaction and the phase relations between the quasiparticle density oscillations in components (16) [see also Fig. 1a,b] guarantee its cancellation in the total force

$$\mathcal{F}_{\omega\mathbf{k}}^\alpha = -i\mathbf{k} \left( f_0^{\alpha\alpha} - \frac{e_\alpha}{e_\beta} f_0^{\alpha\beta} \right) \delta N_s^{(\alpha)}, \quad \alpha \neq \beta. \quad (53)$$

Note that the total restoring forces in the acoustic plasmon mode are determined by the short-range quasiparticle interaction just like the case of conventional zero sound in single-component neutral Fermi liquids. According to Eqs. (52) and (53), intracomponent short-range attraction counteracts the long-range electrostatic repulsion while the intercomponent short-range interaction is responsible for the established charge asymmetry.

Isotropic attractive short-range interaction reduces the effective interaction parameter (18) in comparison to the

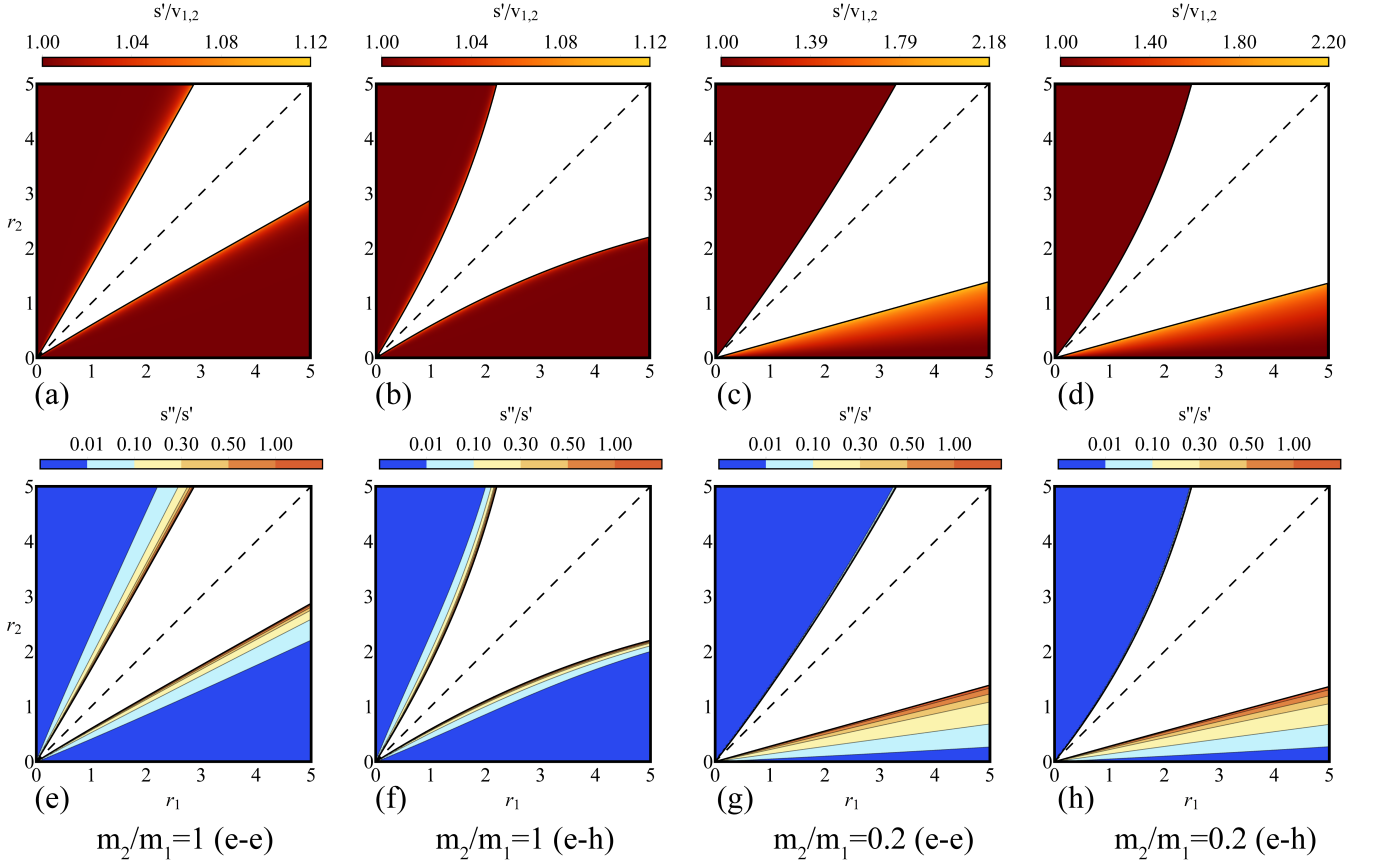


FIG. 7. Diagrams of acoustic plasmon velocity (a-d) and damping (e-h) in three-dimensional two-component electron-electron and electron-hole liquids with equal and strongly different masses in components.

RPA case  $F_{\text{eff}} < F_{\text{RPA}}$ . Consequently, one could expect the reduction of the acoustic plasmon velocity  $s' < s'_{\text{RPA}}$  and the increase of damping  $s'' > s''_{\text{RPA}}$  in two-component electron liquids. This is consistent with the results of calculation performed in [33, 44] for electron-hole liquids within the generalized RPA. This procedure is equivalent to using the Eq. (11) for the acoustic plasmon dispersion with the approximate reduced Landau parameters  $\tilde{F}_0^{\alpha\alpha} = -\frac{2}{\pi}\gamma_d r_\alpha$  when the form of the static local field factors is chosen to satisfy the compressibility sum rule.

The behavior of the microscopically calculated isotropic Landau parameters is more complicated. In three dimensions the main effect of the short-range interaction is the reconstruction of the forbidden domain at  $r_1 \sim r_2$ , where the strength of the short-range interaction grows with  $\rho_s = \sqrt{r_1^2 + r_2^2}$ . In the quasi single-component domains both  $F_{\text{RPA}}$  and  $F_0^{\alpha\beta}$  are small due to strong screening by high-density component and the effect of renormalization is minimal: ion-acoustic wave regime is still suppressed (like in RPA) and the well-defined acoustic plasmon propagates in the weakly interacting regime at  $r_2 \ll r_1$  and  $r_2 \gg r_1$  independently on the mass ratio, see Fig. 7.

In two dimensions, the effects of charge asymmetry and the reconstruction of the forbidden domain are more

prominent (see Fig. 8) than in 3D since  $F_{\text{RPA}}$  is constant. The variation of acoustic plasmon velocity with  $r_{1,2}$  is determined by the behavior of the isotropic Landau parameters in the  $r_1 - r_2$  plane. The renormalization of the acoustic plasmon mode is minimal, like in 3D, since the domains where the mode is well-defined coincide with the regions of strong screening. Pines plasmon can propagate in 2D two-component electron liquids with the strong mass difference when the heavier component is the slowest and the weakly interacting propagation regime is realized when it is the fastest.

The values of the isotropic Landau parameters used to establish the renormalization of the acoustic plasmon mode were calculated in Section IV in the random-phase approximation, which is exact only in the high density domains  $r_{1,2} \ll 1$ . The higher quantitative accuracy can be achieved by the quantum Monte Carlo (QMC) or generalized RPA (GRPA) calculations [49]. However, the former are rather complicated while the accuracy of the latter strongly depends on the approximations used for the local field factors [49] and their generalization for the two-component case is the subject of the separate work. However, we stress that the calculated diagrams in 3D and 2D describe the actual picture qualitatively well and the main results of this section, namely, charge asym-

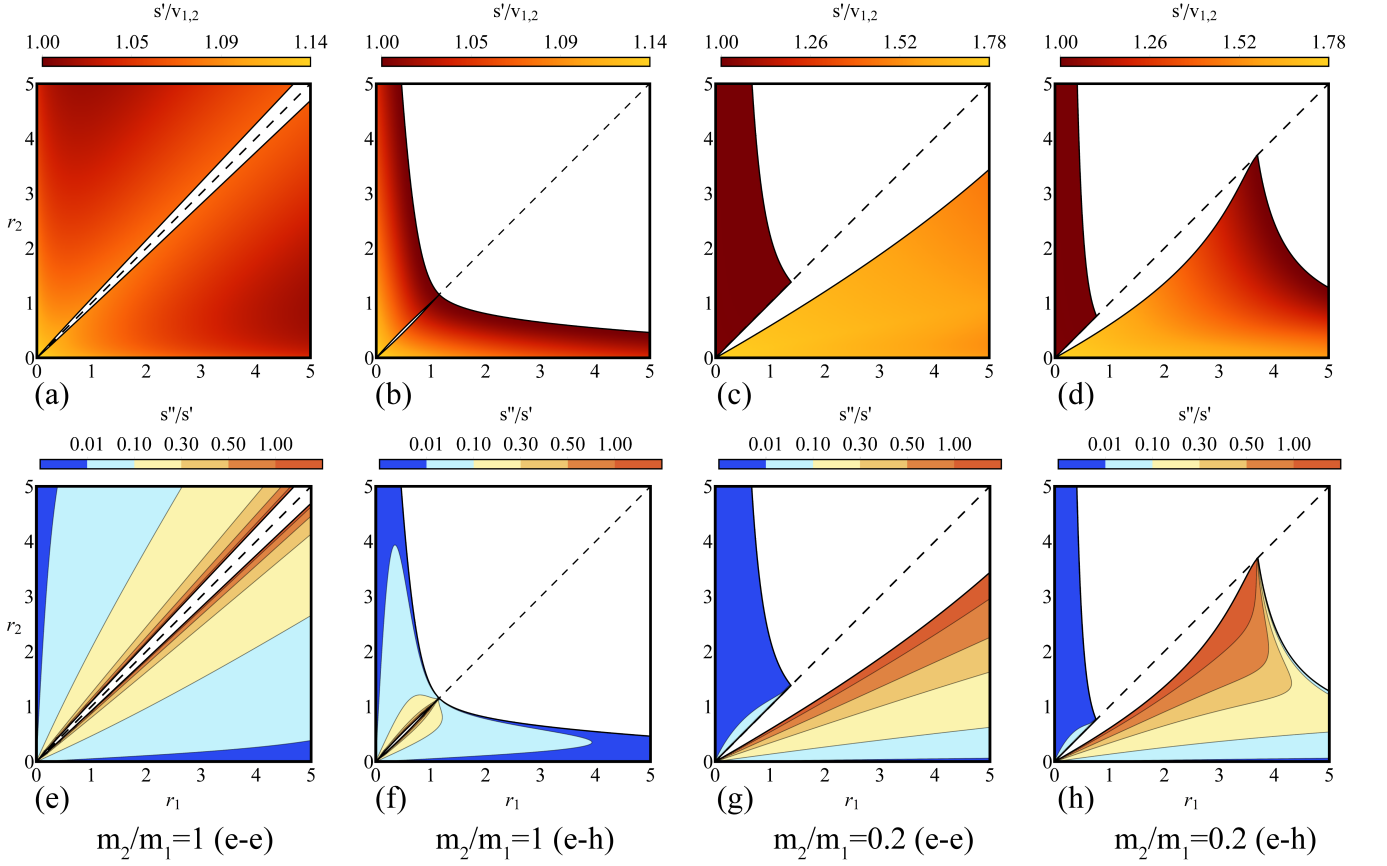


FIG. 8. Diagrams of acoustic plasmon velocity (a-d) and damping (e-h) in two-dimensional two-component electron-electron and electron-hole liquids with equal and strongly different masses in components.

metry and the stability of the acoustic plasmon mode to the short-range interaction are valid regardless of the approximation used. In addition to this, an excellent convergence of the RPA and QMC results for the compressibility of three-dimensional electron liquid [58] determined by  $F_0$  indicates that our calculation in 3D can be accurate beyond the high-density domain.

## VI. DISCUSSION AND CONCLUSIONS

The main reason why acoustic plasmons in two-component electron liquids have been attracting significant interest over decades is their ability to mediate the electron-electron interaction in the fast component. The resulting effective interparticle interaction of the Fröhlich type opens up possibilities for the formation of plasmonic superconductivity and the emergence of the acoustic plasmaron [59, 60] features in the single-particle spectrum of the fast component. However, the reliable experimental manifestation of these phenomena is still missing. The strength of the effective electron-electron interaction depends on the electron-acoustic plasmon coupling constant  $|g_k|^2 \sim (s'^2/v_1^2 - 1)^{3/d}$ . Therefore, the abovementioned effects are favorable only if acoustic plas-

mon propagates in the ion-acoustic wave regime, which is similar to the renormalized acoustic phonon in the BCS theory [61]. However, as we have seen above, the Pines plasmon regime is suppressed in 3D and thus the associated Fröhlich-like interaction is missing. In two dimensions, the acoustic plasmon mediated interaction is weak since the corresponding threshold for the effective interaction constant  $F_{\text{eff}} \gg 8$  is hardly achievable in the two-component liquids with parabolic dispersion  $m_2/m_1 \ll 0.1$ .

The most promising platform where both regimes of acoustic plasmon propagation manifest and the mediated electron-electron interaction can be strong enough are anisotropic multivalley semimetals. In these materials, quasiparticles which reside in the vicinity of nonequivalent valleys form the two-component degenerate plasma and the low crystal symmetry leads to the strong anisotropy of its properties. The strong Fermi velocities contrast in different valleys provides the weakly coupled regime of the embodied two-component liquid, making the acoustic plasmon mode equivalent to the zero sound propagating in the slow component. The direct transformation between zero sound in weakly interacting case and the ion-acoustic wave can take place within a single crystal with the change of the wave propaga-

tion direction with respect to the crystallographic axes, as it was recently predicated for the case of type-I Weyl semimetals like TaAs [62] by numerical calculations of the anisotropy of acoustic plasmon velocity. In addition to this, the smallness of the interaction constant averaged over the crystallographic directions ensures the absence of the renormalization effects due to the short-range interaction. Unlike shear sound, acoustic plasmon-zero sound mode in condensed mattes systems is experimentally accessible by the full set of charge-sensitive experimental techniques, e.g. energy-loss spectroscopy and time-resolved measurements of the relaxation of electrostatic perturbations.

## ACKNOWLEDGMENTS

The author is grateful to D. Svintsov, A. A. Greshnov and G. G. Zegrya for valuable discussions and advice.

This work was supported by the Foundation for the

Advancement of Theoretical Physics and Mathematics BASIS (Grant No. 19-1-5-127-1).

## Appendix: Explicit form of the isotropic Landau parameters in three- and two-dimensional two-component electron liquids

At arbitrary values of Wigner-Seitz radii  $r_{1,2}$ , isotropic Landau parameters in two-component electron liquids can be calculated only numerically. The screened exchange term  $F_{\text{SX}}^{\alpha\beta}$  is represented by the one-dimensional integral of (41) over  $\vartheta$ . Angular integrations over directions of  $\mathbf{q}$  and  $\mathbf{k}'$  in the coulomb hole term  $F_{\text{CH}}^{\alpha\beta}$  can be done analytically and independently for the case of isotropic liquid, so that  $F_{\text{CH}}^{\alpha\beta}$  is given by the two-dimensional integral. Explicit expressions for the isotropic Landau parameters have the form

$$F_{0,\text{SX}}^{\alpha\beta} = -\delta_{\alpha\beta} \frac{\gamma_3 r_\alpha}{\pi} \int_0^1 \frac{u du}{u^2 - \frac{\gamma_3 r_\alpha}{\pi} \sum_{j=1,2} \frac{\kappa_j^2}{\kappa_\alpha^2} \tilde{\Pi}_3 \left[ \frac{k_\alpha}{k_j} u, 0 \right]}, \quad (\text{A.1})$$

$$F_{0,\text{CH}}^{\alpha\beta} = -\frac{\gamma_3^2 r_\alpha r_\beta}{4\pi^3} \int_0^{+\infty} du \int_0^{+\infty} dw \frac{u \prod_{j=\alpha,\beta} \mathcal{G}_3 \left[ \frac{k_\beta}{k_j} u, \frac{v_\beta}{v_j} w \right]}{\left( u^2 - \frac{\gamma_3 r_\beta}{\pi} \sum_{j=1,2} \frac{\kappa_j^2}{\kappa_\beta^2} \tilde{\Pi}_3 \left[ \frac{k_\beta}{k_j} u, i \frac{v_\beta}{v_j} w \right] \right)^2}, \quad (\text{A.2})$$

in three dimensions and

$$F_{0,\text{SX}}^{\alpha\beta} = -\delta_{\alpha\beta} \frac{\gamma_2 r_\alpha}{\pi} \int_0^1 \frac{du}{\sqrt{1-u^2}} \frac{1}{u - \gamma_2 r_\alpha \sum_{j=1,2} \frac{\kappa_j}{\kappa_\alpha} \tilde{\Pi}_2 \left[ \frac{k_\alpha}{k_j} u, 0 \right]}, \quad (\text{A.3})$$

$$F_{0,\text{CH}}^{\alpha\beta} = -\frac{\gamma_2^2 r_\alpha r_\beta}{\pi} \int_0^{+\infty} du \int_0^{+\infty} dw \frac{\prod_{j=\alpha,\beta} \mathcal{G}_2 \left[ \frac{k_\beta}{k_j} u, \frac{v_\beta}{v_j} w \right]}{\left( u - \gamma_2 r_\beta \sum_{j=1,2} \frac{\kappa_j}{\kappa_\beta} \tilde{\Pi}_2 \left[ \frac{k_\beta}{k_j} u, i \frac{v_\beta}{v_j} w \right] \right)^2}, \quad (\text{A.4})$$

in two dimensions. Here  $\gamma_3 = (4/9\pi)^{1/3}$  and  $\gamma_2 = 1/\sqrt{2}$ . The dimensionless integration variables stand for  $u = |\mathbf{k}_\alpha - \mathbf{k}'_\alpha|/2k_\alpha$  in the screened exchange terms and for  $u = q/2k_\beta$  and  $w = \omega/v_\beta q$  in the coulomb hole ones. The functions  $\mathcal{G}_d \left( \frac{k}{2k_F}, \frac{\omega}{v_F k} \right) = 2^{\frac{1-d}{4-d}} \frac{k_F}{k} \mu^{-1} \sum_{\Omega_\mathbf{k}} [G(\mathbf{k}_F - \mathbf{k}, \mu - i\omega) + G(\mathbf{k}_F + \mathbf{k}, \mu + i\omega)]$  given by

$$\mathcal{G}_3(u, w) = \ln \frac{(1-u)^2 + w^2}{(1+u)^2 + w^2}, \quad (\text{A.5})$$

$$\mathcal{G}_2(u, w) = - \left( \frac{\sqrt{(u^2 - w^2 - 1)^2 + 4u^2 w^2} + u^2 - w^2 - 1}{(u^2 - w^2 - 1)^2 + 4u^2 w^2} \right)^{1/2}, \quad (\text{A.6})$$

are proportional to the probability amplitudes of excitation of non-interacting fermion from the Fermi surface, averaged over the directions of the wave vector. Dimensionless RPA polarizabilities  $\tilde{\Pi}_d(u, iw)$  at imaginary frequencies are real-

valued functions even in  $\omega$ . They have the form

$$\tilde{\Pi}_3(u, iw) = -\frac{1}{2} + \frac{1-u^2+w^2}{8u} \ln \frac{(1-u)^2+w^2}{(1+u)^2+w^2} + \frac{w}{2} \left( \arctan \frac{1-u}{w} + \arctan \frac{1+u}{w} \right), \quad (\text{A.7})$$

$$\tilde{\Pi}_2(u, iw) = -1 + \frac{1}{\sqrt{2}u} \left( \sqrt{(u^2-w^2-1)^2+4u^2w^2} + u^2-w^2-1 \right)^{1/2}. \quad (\text{A.8})$$

Note that  $\tilde{\Pi}_d(u, iw)$  are strongly non-uniform in the  $(u, w)$  space. Polarizabilities  $\tilde{\Pi}_d(u, iw) \approx -1$  are finite for the electron transitions at the Fermi surface  $0 < u < 1$ ,  $w \ll 1$ . Therefore, the corresponding coulomb interaction is substantially screened. However, the transitions outside the Fermi surface are affected by a rather weak dynamical screening, described by  $\tilde{\Pi}_d(u, iw) \approx -1/d(u^2+w^2)$  at  $u, w \gg 1$ .

---

[1] L. D. Landau, The Theory of a Fermi Liquid, *Zh. Exp. Teor. Fiz.* **30**, 1058 (1956), [*Sov. Phys. JETP* **3**, 920 (1957)].

[2] L. D. Landau, Oscillations in a Fermi Liquid, *Zh. Exp. Teor. Fiz.* **32**, 59 (1957), [*Sov. Phys. JETP* **5**, 101 (1957)].

[3] A. Rodin, M. Trushin, A. Carvalho, and A. H. Castro Neto, Collective excitations in 2D materials, *Nature Reviews Physics* **2**, 524 (2020).

[4] D. Pines, *Elementary Excitations in Solids* (CRC Press, Boca Raton, FL, 2018).

[5] M. Polini and A. K. Geim, Viscous electron fluids, *Physics Today* **73**, 28 (2020).

[6] A. Lucas and K. C. Fong, Hydrodynamics of electrons in graphene, *Journal of Physics: Condensed Matter* **30**, 053001 (2018).

[7] P. J. W. Moll, P. Kushwaha, N. Nandi, B. Schmidt, and A. P. Mackenzie, Evidence for hydrodynamic electron flow in PdCoO<sub>2</sub>, *Science* **351**, 1061 (2016).

[8] G. M. Gusev, A. D. Levin, E. V. Levinson, and A. K. Bakarov, Viscous electron flow in mesoscopic two-dimensional electron gas, *AIP Advances* **8**, 025318 (2018).

[9] D. Svintsov, Hydrodynamic-to-ballistic crossover in Dirac materials, *Phys. Rev. B* **97**, 121405 (2018).

[10] E. I. Kiselev and J. Schmalian, Nonlocal hydrodynamic transport and collective excitations in Dirac fluids, *Phys. Rev. B* **102**, 245434 (2020).

[11] B. N. Narozhny, I. V. Gornyi, and M. Titov, Hydrodynamic collective modes in graphene, *Phys. Rev. B* **103**, 115402 (2021).

[12] I. Torre, L. Vieira de Castro, B. Van Duppen, D. Barcons Ruiz, F. m. c. M. Peeters, F. H. L. Koppens, and M. Polini, Acoustic plasmons at the crossover between the collisionless and hydrodynamic regimes in two-dimensional electron liquids, *Phys. Rev. B* **99**, 144307 (2019).

[13] V. P. Silin, On the Theory of Plasma Waves in a Degenerate Electron Liquid, *Zh. Exp. Teor. Fiz.* **34**, 781 (1958), [*Sov. Phys. JETP* **7**, 538 (1958)].

[14] V. P. Silin, The Oscillations of a Degenerate Electron Fluid, *Zh. Exp. Teor. Fiz.* **35**, 1243 (1959), [*Sov. Phys. JETP* **8**, 870 (1959)].

[15] A. Lucas and S. Das Sarma, Electronic sound modes and plasmons in hydrodynamic two-dimensional metals, *Phys. Rev. B* **97**, 115449 (2018).

[16] S.-K. Jian and S. Das Sarma, Hydrodynamic sound and plasmons in three dimensions, *Phys. Rev. B* **103**, 155101 (2021).

[17] D. Pines and D. Bohm, A Collective Description of Electron Interactions: II. Collective vs Individual Particle Aspects of the Interactions, *Phys. Rev.* **85**, 338 (1952).

[18] L. P. Gor'kov and I. E. Dzyaloshinskii, Feasibility of Zero-sound Oscillations in Metals, *Zh. Exp. Teor. Fiz.* **44**, 1650 (1963), [*Sov. Phys. JETP* **17**, 1111 (1963)].

[19] A. Klein, D. L. Maslov, L. P. Pitaevskii, and A. V. Chubukov, Collective modes near a Pomeranchuk instability in two dimensions, *Phys. Rev. Research* **1**, 033134 (2019).

[20] R. Aquino and D. G. Barci, Two-dimensional Fermi liquid dynamics with density-density and quadrupolar interactions, *Phys. Rev. B* **100**, 115117 (2019).

[21] R. Aquino and D. G. Barci, Exceptional points in Fermi liquids with quadrupolar interactions, *Phys. Rev. B* **102**, 201110 (2020).

[22] P. S. Alekseev, Magnetic resonance in a high-frequency flow of a two-dimensional viscous electron fluid, *Phys. Rev. B* **98**, 165440 (2018).

[23] P. S. Alekseev, Magnetosonic Waves in a Two-Dimensional Electron Fermi Liquid, *Semiconductors* **53**, 1367 (2019).

[24] P. S. Alekseev and A. P. Alekseeva, Transverse Magnetosonic Waves and Viscoelastic Resonance in a Two-Dimensional Highly Viscous Electron Fluid, *Phys. Rev. Lett.* **123**, 236801 (2019).

[25] J. Y. Khoo and I. S. Villadiego, Shear sound of two-dimensional Fermi liquids, *Phys. Rev. B* **99**, 075434 (2019).

[26] Y. Zhang, F. Zhai, and W. Jiang, High-frequency magnetotransport in a viscous electron fluid under a Stern-Gerlach force, *Phys. Rev. B* **104**, 165139 (2021).

[27] J. Y. Khoo, P.-Y. Chang, F. Pientka, and I. Sodemann, Quantum paracrystalline shear modes of the electron liquid, *Phys. Rev. B* **102**, 085437 (2020).

[28] D. Valentini, J. Zaanen, and D. van der Marel, Propagation of shear stress in strongly interacting metallic Fermi liquids enhances transmission of terahertz radiation, *Sci. Rep.* **11**, 7105 (2021).

[29] D. Valentini, Optical signatures of shear collective modes in strongly interacting Fermi liquids, *Phys. Rev. Research* **3**, 023076 (2021).

[30] L. D. Landau, E. M. Lifshitz, and L. P. Pitaevskii, *Course of Theoretical Physics: Statistical Physics, Part 2*, Vol. 9 (Pergamon, Oxford, 1980).

[31] D. Pines, Electron interaction in solids, *Canadian Journal of Physics* **34**, 1379 (1956).

[32] H. Fröhlich, Superconductivity in metals with incomplete inner shells, *Journal of Physics C: Solid State Physics* **1**, 544 (1968).

[33] G. Vignale and K. S. Singwi, Possibility of superconductivity in the electron-hole liquid, *Phys. Rev. B* **31**, 2729 (1985).

[34] G. S. Canright and G. Vignale, Superconductivity and acoustic plasmons in the two-dimensional electron gas, *Phys. Rev. B* **39**, 2740 (1989).

[35] V. Fatemi and J. Ruhman, Synthesizing Coulombic superconductivity in van der Waals bilayers, *Phys. Rev. B* **98**, 094517 (2018).

[36] J. Ruhman and P. A. Lee, Pairing from dynamically screened Coulomb repulsion in bismuth, *Phys. Rev. B* **96**, 235107 (2017).

[37] G. Sharma, M. Trushin, O. P. Sushkov, G. Vignale, and S. Adam, Superconductivity from collective excitations in magic-angle twisted bilayer graphene, *Phys. Rev. Research* **2**, 022040 (2020).

[38] A. Agarwal, M. Polini, G. Vignale, and M. E. Flatté, Long-lived spin plasmons in a spin-polarized two-dimensional electron gas, *Phys. Rev. B* **90**, 155409 (2014).

[39] D. Kreil, R. Hobbiger, J. T. Drachta, and H. M. Böhm, Excitations in a spin-polarized two-dimensional electron gas, *Phys. Rev. B* **92**, 205426 (2015).

[40] Y. M. Xiao, W. Xu, F. M. Peeters, and B. Van Duppen, Multicomponent plasmons in monolayer MoS<sub>2</sub> with circularly polarized optical pumping, *Phys. Rev. B* **96**, 085405 (2017).

[41] V. V. Enaldiev, Collective excitations in a two-component one-dimensional massless Dirac plasma, *Phys. Rev. B* **98**, 155417 (2018).

[42] M. Schober, D. Kreil, and H. M. Böhm, Dynamic response of partially spin- and valley-polarised two-dimensional electron liquids, *EPL (Europhysics Letters)* **129**, 17001 (2020).

[43] G. Vignale and K. Singwi, Collective modes in electron-hole liquids, *Solid State Communications* **44**, 259 (1982).

[44] G. Vignale, Acoustic plasmons in a two-dimensional, two-component electron liquid, *Phys. Rev. B* **38**, 811 (1988).

[45] S. Z. Dunin and E. P. Fetisov, Zero sound waves in two-component Fermi liquids, *Fiz. Tverd. Tela* **14**, 270 (1972), [Sov. Phys.-Solid State **14**, 221 (1972)].

[46] I. A. Akhiezer and E. M. Chudnovskii, Theory of a two-component Fermi liquid, *Zh. Exp. Teor. Fiz.* **66**, 2303 (1974), [Sov. Phys. JETP **39**, 1135 (1974)].

[47] J. Oliva and N. W. Ashcroft, Two-component Fermi-liquid theory: Transport properties of liquid metallic hydrogen, *Phys. Rev. B* **25**, 223 (1982).

[48] D. Pines and P. M. Nozières, *The Theory of Quantum Liquids* (CRC Press, Boca Raton, FL, 2018).

[49] G. Giuliani and G. Vignale, *Quantum Theory of the Electron Liquid* (Cambridge University Press, 2005).

[50] A. Y. Romanov, V. P. Silin, and S. A. Uryupin, Transverse zero-sound waves in two-component Fermi liquid, *Bull. Lebedev Phys. Inst.* **35**, 323 (2008).

[51] E. M. Lifshitz and L. P. Pitaevskii, *Course of Theoretical Physics: Physical Kinetics*, Vol. 10 (Pergamon, Oxford, 1981).

[52] Here we assume that the amplitude of the self-consistent potential is real function.

[53] T. Rice, The effects of electron-electron interaction on the properties of metals, *Annals of Physics* **31**, 100 (1965).

[54] L. Hedin, New Method for Calculating the One-Particle Green's Function with Application to the Electron-Gas Problem, *Phys. Rev.* **139**, A796 (1965).

[55] C. S. Ting, T. K. Lee, and J. J. Quinn, Effective Mass and *g* Factor of Interacting Electrons in the Surface Inversion Layer of Silicon, *Phys. Rev. Lett.* **34**, 870 (1975).

[56] S. Yarlagadda and G. F. Giuliani, Landau theory of Fermi liquids and the integration-over-the-coupling-constant algorithm, *Phys. Rev. B* **49**, 14172 (1994).

[57] In this work we use the following definitions of the complete elliptic integrals:  $K(m) = \int_0^{\pi/2} (1 - m \sin^2 \theta)^{-1/2} d\theta$  and  $E(m) = \int_0^{\pi/2} (1 - m \sin^2 \theta)^{1/2} d\theta$ .

[58] G. E. Simion and G. F. Giuliani, Many-body local fields theory of quasiparticle properties in a three-dimensional electron liquid, *Phys. Rev. B* **77**, 035131 (2008).

[59] B. I. Lundqvist, Single-particle spectrum of the degenerate electron gas, *Phys. kondens. Materie* **6**, 193 (1967).

[60] A. Principi, R. Asgari, and M. Polini, Acoustic plasmons and composite hole-acoustic plasmon satellite bands in graphene on a metal gate, *Solid State Communications* **151**, 1627 (2011).

[61] R. D. Mattuck, *A Guide to Feynman Diagrams in the Many-Body Problem* (Dover Publications, Mineola, N.Y., 1992).

[62] A. N. Afanasiev, A. A. Greshnov, and D. Sintsov, Acoustic plasmons in type-I Weyl semimetals, *Phys. Rev. B* **103**, 205201 (2021).